Chemical Engineering Journal 120 (2006) 127–132

Chemical Engineering Journal

www.elsevier.com/locate/cej

# A comparison of catalyst deactivation of vanadia catalysts used for alkane dehydrogenation

S. David Jackson [a,*], Sreekala Rugmini [a], Peter C. Stair [b,c], Zili Wu [b]

[a] *WestCHEM, Department of Chemistry, University of Glasgow, Glasgow G12 8QQ, United Kingdom*
[b] *Department of Chemistry, Northwestern University, IL 60208, United States*
[c] *Argonne National Laboratory, Argonne, IL 60439, United States*

**Abstract**

A series of vanadia/θ-alumina catalysts have been prepared, characterised and tested for *n*-butane dehydrogenation. We examined two catalysts having vanadium loadings of 1 and 3.5% V in more detail. The extent of carbon laydown is extremely sensitive to the nature of vanadia surface species. Studies show that the isolated $VO_x$ species are much more effective at catalysing carbon deposition during dehydrogenation than the polyvanadate species. It is also clear that polyvanadate species are more effective at dehydrogenation compared to the isolated vanadia species.


*Keywords:* Vanadia catalysts; *n*-Butane dehydrogenation; Deactivation; Nature of carbon species; UV–vis. Raman spectra

## 1. Introduction

The catalytic dehydrogenation of lower paraffins, olefins and alkylaromatic hydrocarbons has the highest throughputs in the world chemical industry. The main interest is devoted to the dehydrogenation of *n*-butane to butenes and butadiene, which are precursor molecules for manufacturing synthetic rubber. Supported vanadia catalysts are known to be selective catalysts in a number of catalytic reactions including direct and oxidative dehydrogenation of lower alkanes [1–4]. The process is highly complex with a series of competing side reactions occurring simultaneously leading to significant carbon laydown resulting in catalyst deactivation. Thus, coking, or the formation of carbonaceous deposits formed by oligomerisation of olefins and/or polyalkylation/condensation of aromatics, is an important side reaction in the dehydrogenation process that leads to catalyst deactivation [5–7]. The accurate characterisation of surface carbon is always difficult because of the variety of species that may be present at any one time. Further, the dispersion and morphology of vanadia species have a large effect on coke deposition. Depending on the oxide carrier and $VO_x$ loading, these catalysts exhibit different catalytic pattern and the difference in catalytic behaviour has been attributed to modifications of the nature of surface vanadia species [8–10]. The molecular structures of surface vanadia species have been extensively investigated in the past few years with many different methods [11–14].

The aim of the present paper is to compare catalyst deactivation of vanadia on alumina catalysts with different vanadia loadings. A series of catalysts have been prepared and characterised by UV–vis excited Raman spectroscopy [15]. At lower vanadia loadings, monovanadate is the main surface species. When the vanadia loading is between 1.2 and 4 V/nm$^2$, polyvanadates are characterised on the surface. At surface density above 4 V/nm$^2$, crystalline $V_2O_5$ is formed on the alumina surface. The catalysts, 1 and 3.5% V supported on θ-alumina, were evaluated for *n*-butane dehydrogenation activity and studies were carried out with a view to understand structure–reaction–deactivation relationship.

## 2. Experimental

### 2.1. Preparation of catalysts

All the catalysts were prepared by incipient wetness impregnation as reported earlier [15]. Aqueous $NH_4VO_3$ (>99%, Aldrich) solution was used to prepare the catalysts with lower metal loadings (0.01–1.2% $V_2O_5$ on alumina). Oxalic acid (99%, Aldrich) ($NH_4VO_3$/oxalic acid = 0.5 M) was added into the solutions for high $VO_x$ loadings (4.4–14.2% $V_2O_5$ on alumina) to ensure the dissolution of $NH_4VO_3$. Support used is θ-alumina (Johnson Matthey, UK, 1/20″ trilobes, surface

* Corresponding author.
*E-mail address:* sdj@chem.gla.ac.uk (S.D. Jackson).

1385-8947/$ – see front matter © 2006 Elsevier B.V. All rights reserved.
doi:10.1016/j.cej.2006.03.014

area = 101 $m^2\ g^{-1}$, pore volume = 0.60 ml $g^{-1}$). After impregnation, the samples were mixed thoroughly using a rotavap for 2 h at 350 K to confirm uniform distribution of vanadia precursor on the support alumina and dried by purging with air at 393 K overnight. Finally the samples were calcined at 823 K for 6 h.

### 2.2. Oxygen uptake measurements

Oxygen uptake measurements were carried out at room temperature and also at 873 K after reducing the catalyst at 873 K using pure $H_2$. After reduction, the catalyst surface was purged with He for 30 min and then pulses of oxygen were introduced at the desired temperature until saturation. The amount of oxygen consumed was monitored using an online thermal conductivity detector connected to the effluent of the reactor. Percentage uptake is expressed as: [O(ads.)/M(catalyst)] × 100 assuming an oxygen to metal stoichiometry equal to 1.

### 2.3. Nitrogen adsorption studies

The surface area and pore volume were determined from the nitrogen adsorption curve determined using Micromeritics Gemini III 2375 Surface Area Analyzer after degassing the samples at 393 K overnight.

### 2.4. Dehydrogenation activity evaluation

The activities of the catalysts were determined using a fixed-bed, continuous-flow, reactor. The catalyst (0.25 $cm^3$) was reduced in pure hydrogen (40 $cm^3\ min^{-1}$) for 1 h at 873 K. The flow was switched to argon and the system purged for 30 min. Then, *n*-butane was introduced at a flow rate of 60 $cm^3\ min^{-1}$ at 873 K (GHSV = 14,400) and atmospheric pressure. Reaction products were analysed at regular intervals using an online GC (Agilent 6890 Series-FID, Varian Chrompack Capillary Column CP7568). Regeneration of the catalysts was carried out using 2% $O_2$/Ar at 873 K. The oxides of carbon produced were monitored by MS.

The conversion and selectivity were calculated (on a carbon basis) from the reaction products (*P*), the total amount of *n*-butane fed to the reactor (*X*) and amount of butane out (*Y*) along with reaction products.

$$\%\text{Conversion} = \left[\frac{(X-Y)}{X}\right] \times 100$$

$$\%\text{Selectivity} = \left[\frac{P}{(X-Y)}\right] \times 100$$

The yield of a specific product was obtained by multiplying the *n*-butane conversion by the corresponding selectivity.

### 2.5. Microanalysis (C and H) of the spent catalysts

Exeter Analytica, Inc., CE-440 Elemental Analyzer was used to determine %C and %H in the catalysts after dehydrogenation activity evaluation.

### 2.6. Raman studies

Both UV (244 nm) and visible (488 nm) Raman spectra of V/alumina samples were collected using the UV-Raman instrument built at Northwestern University [16–18]. The 244 nm line is from a Lexel 95 second harmonic generation (SHG) laser equipped with an intracavity non-linear crystal, BBO (β-barium borate: $BaB_2O_4$), that frequency doubled visible radiation into the mid-ultraviolet region. The 488 nm line is obtained by removing the BBO crystal and replacing the UV output coupler by a visible one in the Lexel 95 SHG laser. Because the grating settings in the spectrometer are optimised for Raman scattering near the 244 nm region, the spectral range for visible Raman (∼260 $cm^{-1}$) study on the same spectrometer is much narrower than that of UV-Raman (∼1500 $cm^{-1}$). Consequently, the spectra obtained using 488 nm excitation are displayed in the range 820–1070 $cm^{-1}$. This region contains the strongest and most informative Raman bands of supported $VO_x$ and provides the best comparison to UV-Raman spectra.

To study the butane dehydrogenation and coke deposition, the sample was first reduced by 5% $H_2/N_2$ at 823 K for 60 min in the fluidised bed reactor and then purged with He for 10 min before exposing to 3% *n*-butane/nitrogen at different temperatures for 30 min. The coked catalyst surface was purged with He for 15 min and cooled to room temperature before spectral measurements were taken.

## 3. Results

The nature of the surface vanadia species was characterised by UV- and visible excited Raman spectroscopy [15]. The characterisation revealed that isolated $VO_x$ species dominated at surface density below 1 V/$nm^2$; polyvanadates coexist with monovanadates at surface densities between 1.2 and 4.4 V/$nm^2$; and $V_2O_5$ formed at surface density higher than 4.4 V/$nm^2$. UV ($\lambda_{excitation}$ = 244 nm) and visible ($\lambda_{excitation}$ = 488 nm) excited Raman spectra of the catalysts are shown in Fig. 1.

To correlate the nature of surface vanadia species and catalyst deactivation, further studies were carried out using 1% V/alumina (isolated surface vanadia species) and 3.5% V/alumina (polyvanadates on the surface). Fig. 2 shows the catalyst deactivation pattern of 1 and 3.5% V/alumina catalysts with respect to time on stream. Turn-over frequencies (TOF, $s^{-1}$) at the start of the dehydrogenation reaction were calculated taking surface oxygen uptake of the reduced catalyst as a measure of surface vanadia dispersion (Table 1). Several reaction–regeneration cycles were performed on 3.5% V/alumina and the catalyst was found to be more stable towards deactivation after the first regeneration. The conversion and

Table 1
Oxygen uptake and turn-over frequencies

| | 1% V/$Al_2O_3$ | 3.5% V/$Al_2O_3$ |
|---|---|---|
| Surface uptake, μmol $g^{-1}$ (%), at 300 K | 11.09 (11.0) | 37.74 (11.0) |
| Bulk uptake, μmol $g^{-1}$ (%), at 873 K | 58.5 (60.0) | 408.8 (122.0) |
| TOF, $s^{-1}$ | $1.9 \times 10^{-2}$ | $4.5 \times 10^{-2}$ |

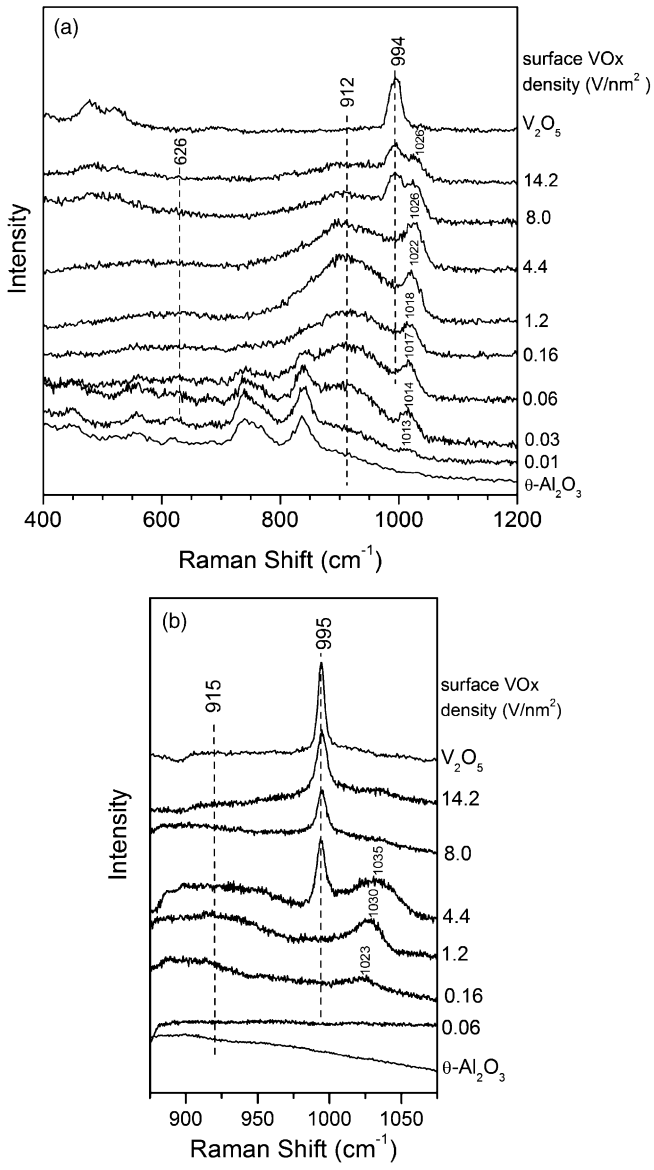


Fig. 1. UV (a) and visible (b) excited Raman spectra of the catalysts.

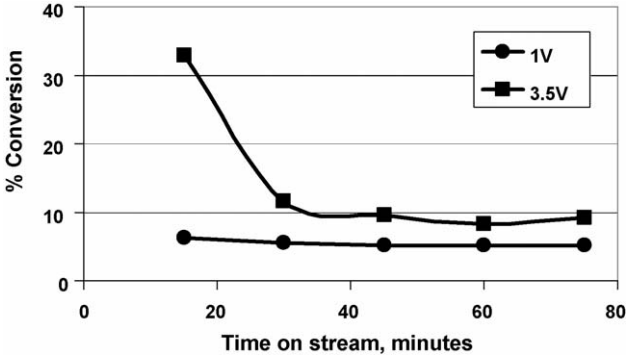


Fig. 2. *n*-Butane dehydrogenation activity of the catalysts.

Table 2
Conversion and selectivities after 60 min on stream

| Catalyst | Conversion (%) 873 K, 60 min | Selectivity (%) | | Yield, butenes (%) |
|---|---|---|---|---|
| | | Carbon | Butenes | |
| 1% V/alumina | 4 | 60 | 20 | 0.8 |
| 3.5 V/alumina | 8 | 38 | 47 | 4 |

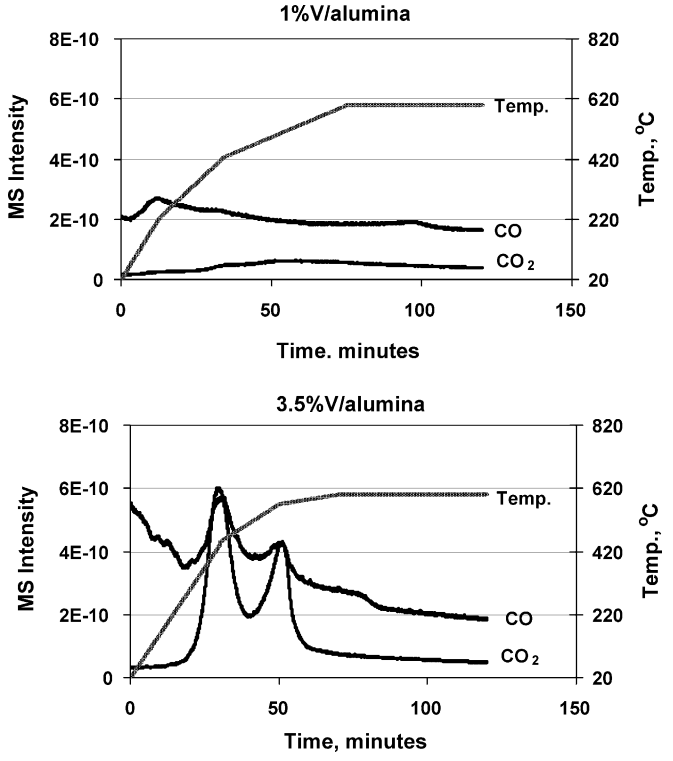


Fig. 3. Temperature programmed oxidation of the carbon species.

selectivities to butenes and carbon species after 60 min on-stream are shown in Table 2. The catalysts were regenerated and the TPO patterns show different types of carbon species on the surface (Fig. 3). The surface areas and pore volume of fresh and coked catalysts, determined from the $N_2$ adsorption curve, are presented in Table 3.

Raman spectroscopic studies and CH microanalyses of the spent catalysts were carried out to examine the topology of carbon species formed during the dehydrogenation process. The percentage carbon, percentage hydrogen and C:H ratio in the spent catalysts are given in Table 4. Fig. 4 shows the growth of carbon species on the catalyst surface during the dehydrogenation process. Fig. 5 gives a comparison of the

Table 3
Nitrogen adsorption data

| Catalyst | Surface area, m$^2$/g (BET method) | Pore volume, ml/g (BJH method) |
|---|---|---|
| 1% V/alumina fresh | 103.5 | 0.49 |
| 3.5% V/alumina fresh | 93.6 | 0.45 |
| 1% V/alumina spent | 109.4 | 0.47 |
| 3.5% V/alumina spent | 94.8 | 0.43 |

Table 4
Microanalysis data of spent catalysts

| Spent catalyst | %C | %H | C:H |
|---|---|---|---|
| 1% V/alumina | 2.3 | 0.2 | 0.9 |
| 3.5% V/alumina | 4.2 | 0.1 | 3.5 |

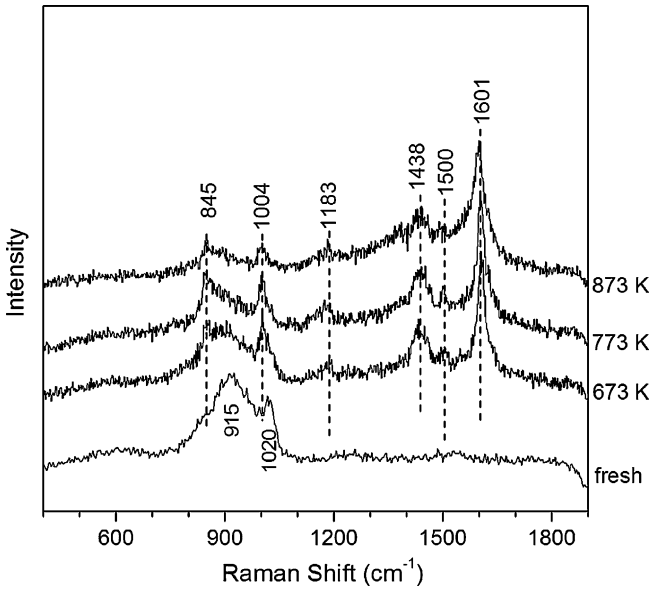


Fig. 4. Raman spectra during dehydrogenation of *n*-butane using 1% V/alumina catalyst.

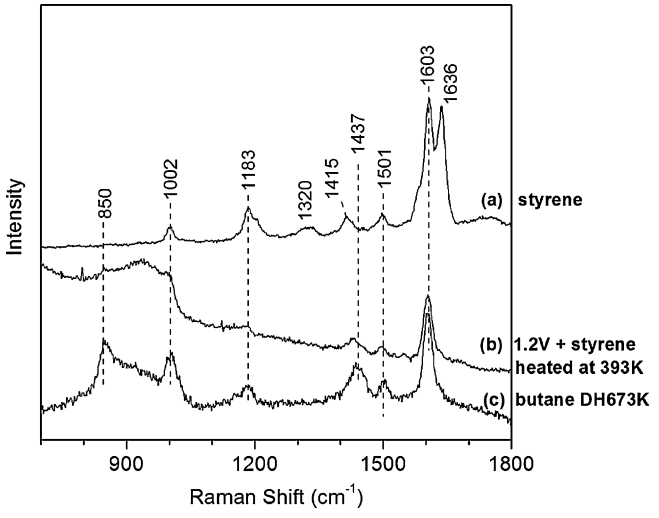


Fig. 5. Raman spectra of polystyrene and coked catalyst.

Raman spectra of the coked catalyst with that of styrene/polystyrene.

## 4. Discussion

The basic alkane dehydrogenation reaction is accompanied by various side reactions, comprising essentially the cracking of feed hydrocarbon to lower hydrocarbons and the formation of dehydrogenated carbonaceous species on the catalyst surface. The formation of this coke leads to the deactivation of the catalyst, and the catalyst requires regular regeneration to restore its activity. The regeneration consists of burning off the coke to re-expose the active sites that have been obscured by the surface deposits. The frequency at which regeneration is required is clearly a function of the rate of activity decline. A main driver in catalyst development is the reduction in deactivation rate.

We have prepared θ-alumina supported vanadia catalysts with different vanadia loadings. The nature of the vanadia species was examined by UV and visible excited Raman spectroscopic studies [15], which suggested that there were three types of vanadia species, monovanadate, polyvanadate and crystalline $V_2O_5$ on the surface of alumina depending upon the vanadia loading (Fig. 1). Isolated vanadia species predominate at surface densities below 1.2 V/nm$^2$, polyvandates are the main surface species at vanadia loadings between 1.2 and 4 V/nm$^2$ and above 4 V/nm$^2$ formation of $V_2O_5$ is observed. In the present study, the catalysts with loadings of 1 and 3.5% V were studied for deactivation during *n*-butane dehydrogenation reaction.

Oxygen uptake at ambient temperature can be taken as a measure of the number of active sites on the catalyst as under these conditions only the surface sites will be re-oxidised. In both catalysts the surface up-take is 11% (Table 1), suggesting a similar dispersion of active sites, although a much smaller number on the 1% catalyst. The bulk re-oxidation figures allow the determination of an average vanadium oxidation state when the catalyst is reduced. The average oxidation state of the 1% $VO_x$/alumina was calculated at 3.8, whereas the average oxidation state for the 3.5% $VO_x$/alumina was calculated at 2.6. These results suggest that the 1% catalyst containing principally isolated vanadate species is harder to reduce than the catalyst containing polyvanadates.

Dehydrogenation activity was studied for the conversion of *n*-butane to butenes. The profile of activity with time on stream is shown in Fig. 2. The conversion and selectivities to butenes and carbon species after 60 min on stream are shown in Table 2. It is clear that the extent of the carbon laydown is extremely sensitive to the nature of vanadia surface species. The isolated surface vanadia species (1% V/alumina) has a far higher selectivity to carbon formation than the polyvanadate surface species (3.5% V/alumina).

Turn-over frequency at the start of the dehydrogenation reaction was calculated taking surface oxygen uptake (%) of the reduced catalyst as a measure of the surface active sites. TOF ($s^{-1}$, based on the analysis at 15 min) for 1% $VO_x$/alumina and 3.5% $VO_x$/alumina catalysts are $1.9 \times 10^{-2}$ and $4.5 \times 10^{-2}$, respectively. This suggests that the polyvanadate species are more effective at dehydrogenation than the isolated $VO_x$ species. This may be a function of the ease of reduction [19,20].

The surface area and pore volumes of the fresh and spent catalysts were determined from the nitrogen adsorption curve by the Brunauer–Emmet–Teller (BET) method and Barrett-Joyner–Hallender (BJH) method, respectively (Table 3). There is no drop in surface area or pore volume during dehydrogenation of *n*-butane which shows that the deactivation is not via

pore blockage or support sintering. Thus, the main cause of deactivation is by the formation of carbanaceous layer on the active sites on the catalyst surface.

In general, dehydrogenation reactions suffer from formation of carbon species where olefins or aromatics are intermediates. At first, a film of paraffinic $–CH_2$-chains is formed, which is then slowly transformed into less reactive polyaromatic or polyolefinic deposits [21–23]. In the present study, an attempt has been made to characterise the coke deposits on the surface by microanalysis of the spent catalyst, temperature programmed oxidation (TPO) and in situ Raman spectroscopic studies. Spent catalysts, after *n*-butane dehydrogenation activity evaluation, were analysed for total C and H content and the results are given in Table 4. The C:H ratio of 1% V/alumina catalyst after evaluation was found to be 0.9, which is very close to that of a polystyrene monomer (see below). But, the C:H ratio for the 3.5% V/alumina spent catalyst is much higher which suggests the presence of highly carbonaceous polyaromatic or graphitic carbon on the surface.

After *n*-butane dehydrogenation reaction, the catalysts were cooled to room temperature and TPO was carried out using 2% $O_2$/Ar and the oxides of carbon coming out are monitored using an online MS. The TPO curves of the spent catalysts are shown in Fig. 3. The profiles show that there are different types of carbon species on the surface causing deactivation of the catalysts and the complete regeneration is complete in two hours. The TPO of the 1% catalyst shows production of CO at 498 and 698 K. The $CO_2$ profile reveals small peaks at 498 and 698 K but the main $CO_2$ production is a broad band centred around 800 K. The TPO of the 3.5% catalyst by contrast has two well-defined $CO_2$ evolutions at 723 and 843 K. Hence, the 3.5% catalyst produces a carbon deposit more resistant to oxidation. This is in agreement with the microanalytical data, which revealed that the deposit on the 3.5% V/alumina catalyst was more hydrogen deficient and hence may be expected to be more difficult to combust.

To study the different types of carbon species formed on the surface, in situ Raman spectroscopic studies were carried out in a fluidised bed arrangement detailed elsewhere [24]. During *n*-butane dehydrogenation reaction, characteristic Raman bands due to deposition of carbon species appear in the region 840–1700 $cm^{-1}$. Typical Raman spectra showing the growth of surface carbon species on the 1% V/alumina catalyst at different temperatures are shown in Fig. 4. An intense band that appears at 1601 $cm^{-1}$ during dehydrogenation can be assigned to C=C stretching in styrene/polystyrene whereas the band at 1500 $cm^{-1}$ is assigned to conjugated polyolefins or cyclopentadienyl species [25,26]. Raman bands at 1020 $cm^{-1}$ and 915 $cm^{-1}$ due to surface $VO_x$ species (V=O and V–O–Al modes of vibration) are slightly shifted to lower energies and is attributed to the binding of carbon species on V. The band at 1438 $cm^{-1}$ can be assigned to C–H bending mode of carbon species. To confirm the presence of polystyrene, Raman spectra were recorded for styrene and also a mixture of styrene and 1% V/alumina catalyst at 393 K. Fig. 5 shows a comparison of these Raman spectra compared with that of 1%V/alumina after coking. The Raman bands confirm that the carbon species formed on the surface is via a polystyrene type intermediate. Further, it is generally accepted that deposition of coke occurs through progressive dehydrogenation, condensation, polymerisation and cyclisation of hydrogen deficient hydrocarbon species on the surface of the catalyst and the coke precursors are mostly olefins and aromatics [27–29].

## 5. Conclusions

The catalytic behaviour and deactivation of vanadia catalysts depend mainly on the nature of surface vanadia species. Catalysts with different vanadia species on the surface (isolated or polymeric) have been studied for the dehydrogenation of *n*-butane. Results show that polyvandate species are more effective at dehydrogenation than the isolated $VO_x$ species. Growth of carbon species on the surface was monitored using Raman spectroscopy and the nature of carbon species was found to be formed via a polystyrene type intermediate. The extent of carbon deposition is extremely sensitive to the nature of vanadia species and the isolated vanadia species is much more selective towards carbon formation.

## Acknowledgement

This work is supported by ATHENA project, which is funded by Engineering and Physical Sciences Research Council (EPSRC) of the UK and Johnson Matthey plc.

## References

[1] A. Klisinska, A. Haras, K. Samson, M. Witko, B. Grzybowska, J. Mol. Catal. A: Chem. 210 (2004) 87.
[2] A.A. Lemonidou, Appl. Catal. A: Gen. 216 (2001) 277.
[3] J.M. Lopez Nieto, P. Concepcion, A. Dejoz, H. Knozinger, F. Melo, M.I. Vazquez, J. Catal. 189 (2000) 147.
[4] I.E. Wachs, B.M. Weckhuysen, Appl. Catal. A: Gen. 157 (1997) 67.
[5] J.M. McNamara, S.D. Jackson, D. Lennon, Catal. Today 81 (2003) 583.
[6] S.D. Jackson, J. Grenfell, I.M. Matheson, S. Munro, R. Ravel, G. Webb, Stud. Surf. Sci. Catal. 111 (1997) 167.
[7] J.R. Rostrup-Nielsen, Catal. Today 37 (1997) 225.
[8] J. Keranen, A. Auroux, S. Ek, L. Niinisto, Appl. Catal. A: Gen. 228 (2002) 213.
[9] M.L. Ferreira, M. Volpe, J. Mol. Catal. A: Chem. 164 (2000) 281.
[10] M.E. Harlin, V.M. Niemi, A.O.I. Krause, J. Catal. 195 (2000) 67.
[11] J.M. Kanervo, M.E. Harlin, A.O.I. Krause, M.A. Banares, Catal. Today 78 (2003) 171.
[12] T. Ono, Y. Tanaka, T. Takeuchi, K. Yamamoto, J. Mol. Catal. A: Chem. 159 (2000) 293.
[13] M.D. Argyle, K. Chen, A.T. Bell, E. Iglesia, J. Catal. 208 (2002) 139.
[14] B.M. Weckhuysen, D.E. Keller, Catal. Today 78 (2003) 25.
[15] Z. Wu, H.S. Kim, P.C. Stair, S. Rugmini, S.D. Jackson, J. Phys. Chem. B 109 (2005) 2793.
[16] Y.T. Chua, P.C. Stair, I.E. Wachs, J. Phys. Chem. B 105 (2001) 8600.
[17] C. Li, P.C. Stair, Stud. Surf. Sci. Catal. 101 (1996) 881.
[18] P.C. Stair, C. Li, J. Vac. Sci. Technol. A 15 (1997) 1679.
[19] B.M. Weckhuysen, I.E. Wachs, R.A. Schoonheydt, Chem. Rev. 96 (1996) 3327.
[20] X. Gao, I.E. Wachs, J. Catal. 192 (2000) 18.
[21] J.R. Rostrup-Nielsen, in: J.R. Anderson, M. Boudart (Eds.), Catal. Sci. Technol., vol. 5, Springer, Berlin, 1984 (Chapter 1).

[22] J.R. Rostrup-Nielsen, T.S. Christensen, ACS Symp. Ser. 634 (1996) 186.
[23] J.R. Rostrup-Nielsen, P.E. Hojlund Nielsen, in: J. Oudar, H. Wise (Eds.), Deactivation and Poisoning of Catalysts, Marcel Dekker, New York, NY, 1985 (Chapter 7).
[24] Y.T. Chua, P.C. Stair, J. Catal. 196 (2000) 66.
[25] Y.T. Chua, P.C. Stair, J. Catal. 213 (2003) 39.
[26] A. Baruya, D.L. Gerrard, W.F. Maddams, Macromolecules 16 (1983) 578.
[27] E.E. Wolf, F. Alfani, Catal. Rev. Sci. Eng. 24 (1982) 329.
[28] D.L. Trimm, Catal. Rev. Sci. Eng. 16 (1977) 155.
[29] J.M. Parera, N.S. Figoli, E.M. Traffano, J. Catal. 79 (1983) 484.